Electrochimica Acta 121 (2014) 321–327

Contents lists available at ScienceDirect

Electrochimica Acta

journal homepage: www.elsevier.com/locate/electacta

Effect of inorganic additive sodium pyrophosphate tetrabasic on positive electrolytes for a vanadium redox flow battery

Se-Kook Park[a,b], Joonmok Shim[a], Jung Hoon Yang[a], Chang-Soo Jin[a], Bum Suk Lee[a], Young-Seak Lee[b], Kyoung-Hee Shin[a], Jae-Deok Jeon[a,*]

[a] Energy Storage Laboratory, Korea Institute of Energy Research, 152 Gajeongno, Yuseong-gu, Daejeon, 305-343, Republic of Korea
[b] Department of Applied Chemistry and Biological Engineering, BK21-E2 M, Chungnam National University, Daejeon 305-764, Republic of Korea

ARTICLE INFO

Article history:
Received 21 October 2013
Received in revised form
31 December 2013
Accepted 2 January 2014
Available online 15 January 2014

Keywords:
Vanadium redox flow batteries
Sodium pyrophosphate tetrabasic
Inorganic additive
Positive electrolyte
Discharge capacity

ABSTRACT

Sodium pyrophosphate tetrabasic (SPT) is employed as an inorganic additive in the positive electrolyte of a vanadium redox flow battery (VRFB) to improve its long-term stability and electrochemical performance. The results of precipitation tests show that the long-term stability of positive electrolytes (2 MV(V) solution in 4 M total sulfates with 0.05 M SPT additive) is improved compared to the blank one. UV-vis and cyclic voltammetry (CV) measurements also suggest that the addition of SPT can effectively delay the formation of precipitation in positive electrolytes, and no new substances are formed in V(V) electrolytes with SPT. The calcined precipitates extracted from the electrolytes with and without a SPT additive are identified as V_2O_5 by X-ray diffraction (XRD) analysis. A VRFB single-unit cell employing positive electrolytes with an additive exhibits the high energy efficiency of 74.6% at a current density of 40 mA cm^2 at the 500th cycle at 20°C, compared to 71.8% for the cell employing the electrolyte without an additive. Moreover, the cell employing the electrolyte with an additive exhibits less discharge capacity fading during cycling in comparison with the pristine one. The disassembled cell without an additive shows a large number of V_2O_5 precipitation particles on the felt electrode after 500 cycles. Meanwhile, the felt electrode of the cell with an additive has little precipitation. That precipitation gives rise to an imbalance between the positive and negative half-cell electrolytes, which results in a significant capacity loss. The additive has shown positive results under limited laboratory short-term and small-scale conditions.

1. Introduction

Electric energy generated from renewable sources such as wind and solar offers enormous potential for meeting future energy demands [1–3]. However, the use of electricity generated from these random and intermittent renewable sources requires efficient electrical energy storage. Energy storage systems (ESSs) such as chemical energy storage devices (batteries) enable electricity to be stored efficiently in chemicals and then released according to demand [4–6]. Redox flow battery (RFB) has been considered to be one of the most promising large-scale ESSs, owing to its attractive features, such as flexible design, high safety, high efficiency, and long cycle life. The RFB is an electrochemical system that allows energy to be stored in two electrolytes. The electrolytes contain different redox couples with electrochemical potentials sufficiently separated from each other to provide an electrochemotive force, which drives the reduction/oxidation (Redox) reactions needed to charge and discharge the cell.

Among various types of RFBs, an all-vanadium redox flow battery (VRFB) studied by Maria Skyllas-Kazacos in the 1980s is one of the most advanced RFBs. The VRFB has been widely regarded as the most suited option for large energy storage by virtue of using one transition metal (vanadium) in both half-cell electrolytes that overcomes the inherent issue of cross contamination by diffusion of different ions across ion-exchange membrane [7–11]. The VRFB is an electrochemical system using reactions of two redox couples of V^{2+}/V^{3+} in a negative half-cell and VO^{2+}/VO_2^+ in a positive half-cell to perform a reversible conversion between electrical energy and chemical energy. Energy density of the VRFB can be determined by concentration of vanadium ions in electrolytes. Therefore, the electrolyte is one of key components for VRFBs, acting not only as an ion conductor but also as an energy storage medium.

However, poor stability of the electrolytes, especially the positive electrolyte, greatly limits the concentration of redox couples in the electrolyte solution, which significantly affects the performance of VRFBs. In particular, above 40°C, V(V) electrolyte suffers from thermal precipitation [12]. The precipitation may cripple the

* Corresponding author. Tel.: +82 42 860 3023; fax: +82 42 860 3133.
E-mail addresses: jdjun74@kier.re.kr, jdjun74@daum.net (J.-D. Jeon).

0013-4686/$ – see front matter © 2014 Elsevier Ltd. All rights reserved.
http://dx.doi.org/10.1016/j.electacta.2014.01.008

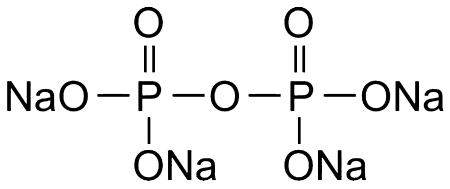

Fig. 1. Molecular structure of sodium pyrophosphate tetrabasic.

pump circulation and severely reduce the efficiency and the capacity of the VRFB and lead to its failure. Thus, it is important to optimize the operating conditions to improve the stability of the electrolyte, especially the positive electrolyte. Much work has been done toward improving the stability of the positive electrolyte. One of the effective methods introduced was to enhance the solubility of the electrolyte solutions, for example, by increasing the concentration of sulfuric acid, H_2SO_4. Higher concentration of sulfuric acid effectively stabilizes V(V) ions but favors the precipitation of V(II), V(III) and V(IV) ions due to the common ion effect [12]. In addition, the increase of acid concentration means higher cost and requires higher corrosive durability for materials. The precipitation can be eliminated over a wider temperature range by reducing vanadium concentration below 2 M, but doing so greatly decreases the energy density of the VRFB. Li and co-workers reported that H_2SO_4-HCl mixture electrolytes exhibited high vanadium concentration (2.5 M) and broad operating temperature (-5 – 50°C) [13]. However, the evolution of Cl_2 gas could be a considerable problem.

Adding precipitation inhibitors is another effective method for stabilizing vanadium electrolytes. A wide range of precipitation inhibitors for V(V) was patented by Skyllas-Kazacos and co-workers and studied in detail as reported earlier [14,15]. Sodium hexametaphosphate ($(NaPO_3)_6$) and alkali metal sulfate were reported to be precipitation inhibitors for supersaturated vanadyl sulfate solutions [16]. These inhibitors can reduce the precipitation rate of the vanadyl sulfate by adsorbing on the surface of the nuclei, thus reducing the rate of crystal growth. Li and co-workers further studied four organic additives proposed by Skyllas-Kazacos and co-workers, including fructose, mannitol, glucose, and d-sorbitol with a positive electrolyte of VRFB [17]. It was confirmed that among them, the electrolyte with d-sorbitol had the best performance, because the active hydroxyl groups (-OH) of d-sorbital not only improve the solubility of the V(V) electrolyte, but also provide more active sites for the V(IV)/V(V) redox reaction. Moreover, it was also reported that organic additives, contained one or more–OH, =O, $-NH_2$, SH groups or combinations of these groups, can encapsulate the hydrate penta coordinated vanadium ion and inhibit their precipitation formation [18].

In this paper, we report in detail our investigation of sodium pyrophosphate tetrabasic (Fig. 1) as an inorganic additive in positive electrolytes for VRFBs and its effect on long-term stability and electrochemical performance, including UV-vis spectrophotometry, cyclic voltammetry (CV), and charge/discharge test. To our knowledge, there are no literature reports on the effect of sodium pyrophosphate tetrabasic containing two phosphate and =O groups on the electrochemical performance of VRFBs.

2. Experimental

The V(IV) electrolyte was prepared by dissolving 2 M $VOSO_4 \cdot 3.5H_2O$ (99.9%, Wako Pure Chemical Industrials, Osaka, Japan) in a sulfuric acid solution containing 4 M total sulfate concentration. Both electrolyte reservoirs initially consisted of a solution containing only the V(IV) ion. The positive and negative electrolyte volumes were 50 mL and 25 mL, respectively. These electrolytes were then charged (cutoff potential: 1.6 V, current density: 5 mA cm^{-2}) until the V(IV) ions were converted to V(V) ions (positive electrode electrolyte) and V(II) (negative electrode electrolyte), and subsequently half of the positive electrolyte solution was removed from its reservoir, making the solution volumes equal (each 25 mL). At the end of the electrolysis, the final solutions were analyzed by redox titration to determine the total vanadium concentration.

To investigate the effects of sodium pyrophosphate tetrabasic (SPT, $Na_4P_2O_7$, ≥ 95%, Sigma-Aldrich) as an inorganic additive on the long-term stability of V(V) electrolytes, sealed samples of electrolytes with and without the SPT additive were stored in a temperature-controlled oven at 20°C until a slight red precipitation visually appeared. The V(V) electrolyte was prepared by dissolving 2 M $VOSO_4 \cdot 3.5H_2O$ in 4 M total sulfates with and without 0.05 M SPT. During the stability test, each sample was monitored twice a day for precipitation. The pristine and stored electrolytes were diluted with 2 M sulfuric acid solution due to sensitivity limitations for measuring UV-vis spectroscopy. The concentration of V(V) ions was determined by UV-vis spectra from a UV-vis spectrophotometer (Optizen 3220UV, Microsys) in the 370 nm to 700 nm wavelength range using a 1.0 cm quartz cell. In order to analyze the composition of the red precipitates extracted from the electrolytes, they were completely dried in air at 520°C for 24 h and characterized by X-ray diffraction (XRD) using a Rigaku-DMax/2500PC (Japan) with Cu-Kα radiation (λ = 1.5406 Å) in the 2θ range from 6 to 50° with 2° min^{-1}. A scanning electron microscope (SEM) (S-4800, Hitachi, Japan) was used to investigate the precipitate morphology.

Cyclic voltammetry (CV) measurements of V(V) solutions with and without the additive were carried out on an electrochemical workstation (Autolab PGSTAT-302 N, EcoChemie, Netherlands) at a scan rate of 100 mV s^{-1} in a potential range of -0.6–1.8 V at 20°C. The curves of current density versus potential were recorded in a three-electrode electrochemical cell with a Pt wire as a counter electrode, silver/silver chloride (Ag/AgCl) as a reference electrode, and a freshly-polished 3 mm diameter glassy carbon as a working electrode.

The VRFB cell performance was tested using an in-house designed non-flow cell system. As shown in Fig. 2, the VRFB single-unit cell was composed of a symmetric structure consisting of two copper current collectors, two graphite bipolar plates (2 mm, Morgan Korea Co., Ltd.), two polypropylene frames, PVC gasket materials, two carbon felt electrodes (4 mm, XF-30A, Toyobo Co., Ltd.) with an effective reaction area of 12 cm^2, and a perfluorinated ion-exchange membrane (GEFC-10 N, thickness = 127 um, Golden Energy Fuel Cell, China). The membrane was used as received without any treatments. The carbon felt electrodes were adjusted to a compression of 25% by stacking pieces of PVC gaskets. This implies that the thickness (3 mm) of half-cell cavity was reduced compared to that (4 mm) of a single carbon felt electrode. Small volumes (ca. 3 mL) of 2 MV(IV) solution in 4 M total sulfates with/without 0.05 M SPT and 2 MV(III) solution in 4 M total sulfates without SPT were injected into the single-unit cell for positive and negative electrolytes, respectively.

The charge/discharge test was conducted between 0.8 V and 1.6 V under a constant current mode at a current density of 40 mA cm^{-2} at 20°C for 500 cycles using a battery cycler (Maccor 4000 Series). Coulombic efficiency (CE), voltage efficiency (VE), and energy efficiency (EE) of the VRFB cell were calculated as in the following equations [19]:

$$CE = (discharge\ capacity / charge\ capacity) \times 100 \quad (1)$$

$$VE = (middle\ point\ of\ discharge\ potentiel / middle\ point\ of\ charge\ potential) \times 100 \quad (2)$$

$$EE = CE \times VE \quad (3)$$

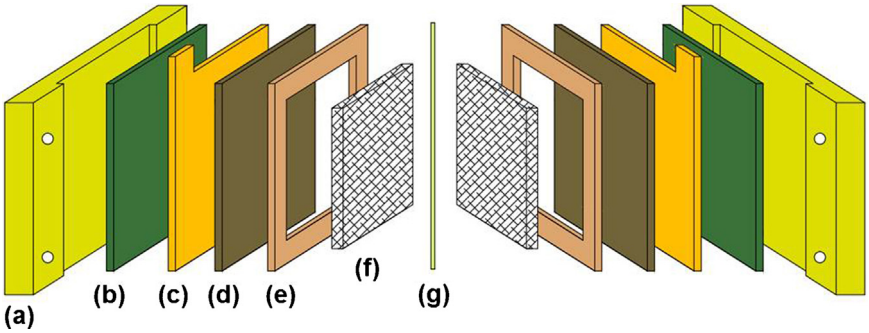

Fig. 2. Schematic diagram of a single non-flow cell: acrylic endplate (a), Viton® gasket (b), copper current collector (c), graphite polar plate (d), polypropylene manifold frame (e), carbon felt electrode (f), and ion exchange membrane (g).

Cell resistance was calculated from Eq. (4) for the discharge obtained from the cell potential and the open circuit potential (OCP) [20];

$$R_D = (E_M - E_D)/I_D \quad (4)$$

where R_D [Ω] is the cell resistance for discharge, E_M is the OCP at the rest time potential between charge and discharge, E_D [V] is the cell potential for the discharge, and I_D [A] is the current during discharge.

3. Results and discussion

3.1. Effect of the additive on the UV-vis and CV of V(V) electrolyte

UV-vis spectrophotometry is an effective analytical technique for vanadium concentration because the color of the vanadium electrolyte changes depending on its oxidation or precipitation state [21]. In order to determine the concentration of V(V) electrolytes, standard solutions with concentrations from 0.02 M to 0.15 M were prepared by diluting a known V(V) electrolyte. Fig. 3(a) shows the UV-vis spectra of the standard solutions of V(V). As shown in the figure, the main absorption peaks of the V(V) ions were observed at wavelengths of ca. 390 nm. The absorbance at the 390 nm is plotted with respect to concentration, thereby drawing a calibration curve (Fig. 3(b)), which shows a linear relationship between the absorbance and concentration in the entire range of concentration. Thus, Beer's law (or Beer-Lambert law) defines a linear relationship between the absorbance and concentration of an absorbing species.

$$A = \varepsilon bC \quad (5)$$

where A is the absorbance, ε is the molar absorptivity, b is the path length through the cell, and C is the concentration. By using the same cuvettes to hold the sample, b is held constant. It was reported that V (V) electrolytes need to be diluted below 0.15 M to quantify the concentration of vanadium ions using the linear relationship between the absorbance and concentrations of an absorbing species [22].

In order to verify precipitation of V(V) ions during storage, the V(V) electrolyte samples with and without a 0.05 M SPT additive were poured into vials and stored in a temperature-controlled oven at 20°C. As the pictures of vials show in Fig. 4, the V(V) electrolyte samples with and without an additive started to precipitate after 24 and 6 days, respectively.

To further measure quantity of the precipitate of the electrolyte samples, the UV-vis spectrophotometer was used. The electrolyte samples were diluted to 1/20 v/v% (V (V) solution: 2 M total sulfates = 1: 20) for UV-vis spectrophotometry analysis to obey Beer's law. Fig. 4(a) shows the UV-vis spectra for pristine and 6 days-stored V(V) electrolytes without a SPT additive. The absorption peaks, λ_{max} of both samples lie at ca. 390 nm, but the absorbance value, A_{max} of the 6 days-stored sample is significantly decreased. The concentration of diluted V(V) ions calculated from Beer's law is 0.082 M (estimated concentration of the undiluted sample: 1.64 M), implying that 0.018 MV(V) ions (estimated concentration of the undiluted sample: 0.36 M) were lost after 6 days.

As seen in Fig. 4(b), the V(V) electrolyte sample with the SPT additive exhibited neither a new absorption peak nor a wavelength shift compared with the pristine sample. This result proves that the addition of a SPT additive does not form a new substance in a positive electrolyte. Further, the concentration of the 24 days-stored sample is 0.083 M (estimated concentration of the undiluted sample: 1.66 M). This concentration value is nearly the same as the 6 days-stored sample without an additive, implying that the addition of SPT can effectively delay the formation of precipitation in positive electrolytes.

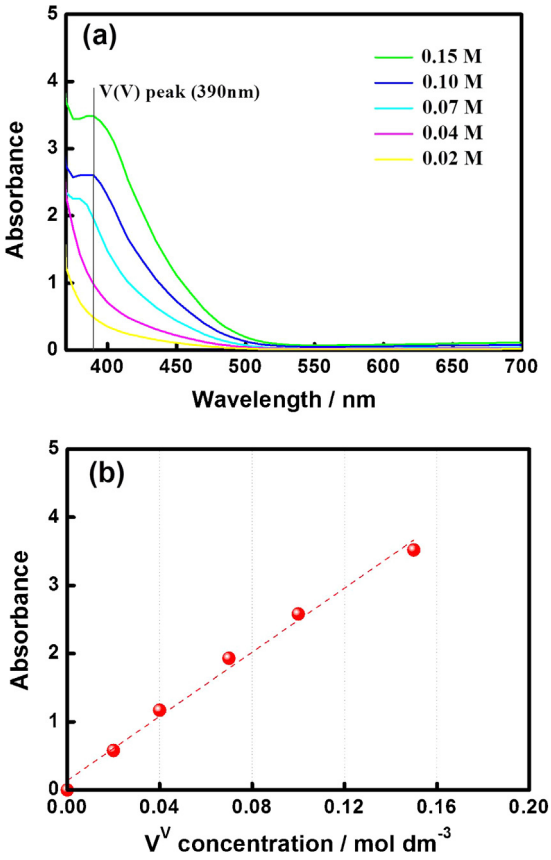

Fig. 3. UV-vis spectra of standard solutions with different vanadium concentrations (a), Beer's law plot (b).

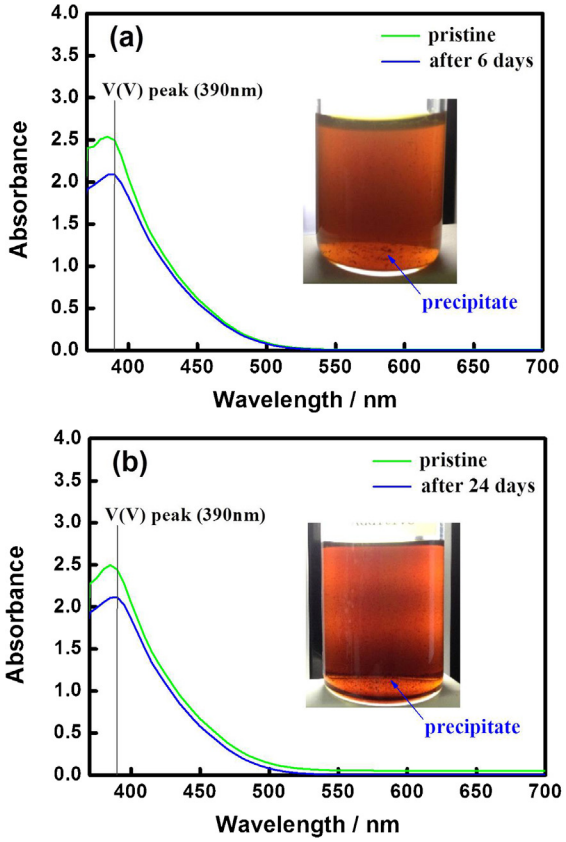

Fig. 4. UV-vis spectra of diluted V(V) solution without (a) and with (b) a SPT additive. The insert images are pictures of precipitate after 6 (a) and 24 (b) days.

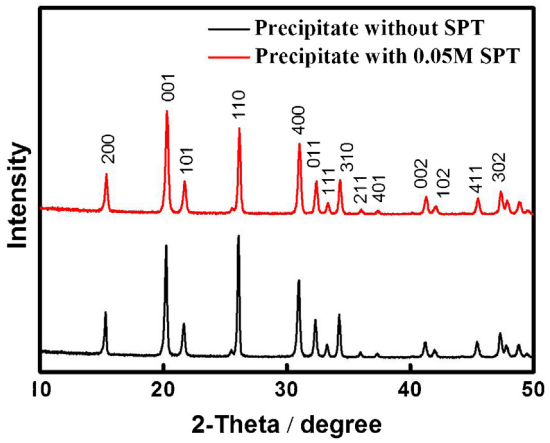

Fig. 5. XRD patterns of precipitates extracted from the electrolytes with and without a SPT additive.

In general, the fully charged V(V) electrolyte exhibits poor stability at high vanadium concentrations (> 2 M) as well as at elevated temperature (> 310 K) [22,23]. This poor stability is due to the precipitation of hydrated V_2O_5 [9,16]. Skyllas-Kazacos and co-workers reported that fully charged positive electrolytes containing 2 MV(V) in 2 M H_2SO_4 and 3 M H_2SO_4 exhibited a slight precipitate in solution at 40°C after 1 day and 2 days, respectively. The increased stability at higher H_2SO_4 concentration is due to the presence of more H^+ ions, which favors the following reaction in the forward direction [23,24].

$$V_2O_5(c) + 2H^+ \Leftrightarrow 2VO_2{}^+ + H_2O \quad (6)$$

Thus, a higher H_2SO_4 concentration is beneficial for redox flow cell applications because it improves the stability of V(V) and increases conductivity. However, H_2SO_4 concentration is limited by the stability of V(IV) species at lower temperatures. Once a precipitate is formed at elevated temperature and/or at high vanadium concentration, it can not change back to V(V) ions, and thereby leads to energy loss and failure of the battery.

The phases of precipitates were determined by XRD. The powder X-ray diffraction of the red precipitates dried at room temperature showed a few broad peaks. However, as shown in Fig. 5, when the precipitates were heated at 520°C, X-ray diffraction patterns with more sharp peaks were observed. These diffraction patterns of the calcined precipitates extracted from the electrolytes with and without a SPT additive correspond well to the V_2O_5. The peaks can be assigned to the orthogonal symmetry of V_2O_5 (space group: Pmmn, $a = 1.152$, $b = 0.357$, $c = 0.437$ nm), which suggests that water has been removed from the red precipitates after heating [25]. Fig. 6 shows the morphologies of the nanoparticles obtained by calcinating the red precipitates at 520°C. As shown in the SEM images, the particle size of the calcined precipitates extracted from the electrolytes with and without a SPT additive was around 1 μm and they had a rodlike morphology.

Fig. 7 shows the CV behaviors of 2 MV(V) solution in 4 M total sulfates with and without the SPT additive at the working electrode, glassy carbon, during the initial 200 cycles at a scan rate of 100 mV s^{-1}. As the scans proceeded, almost no variation of current responses is observed on the peak shape and the peak potential separation, suggesting that the positive electrolyte with a SPT additive have good cycling stability.

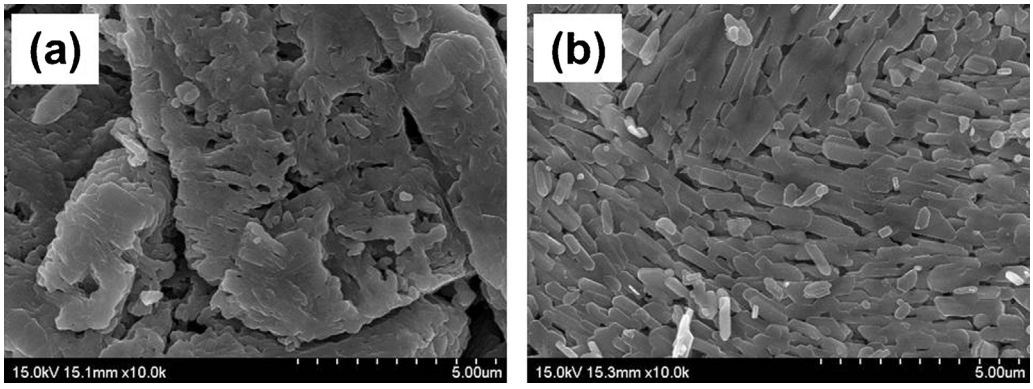

Fig. 6. SEM images of precipitates extracted from the electrolytes with and without a SPT additive.

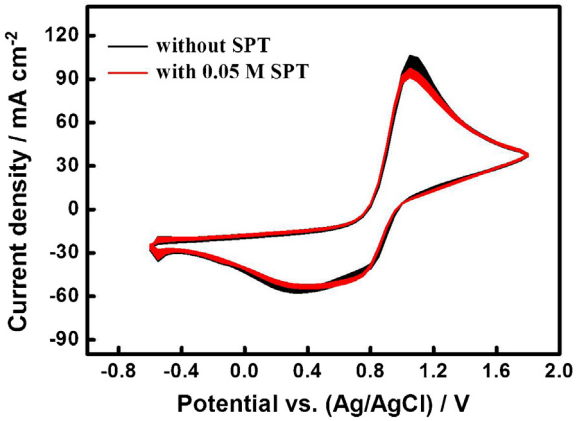

Fig. 7. Cyclic voltammograms (200 cycles) of positive electrolyte solutions with and without a SPT additive.

3.2. Electrochemical performance of VRFB non-flow cells

A charge/discharge test using the in-house designed single-unit cell was performed to further understand the effect of SPT additive in positive electrolytes on the electrochemical performance of VRFB non-flow cells. 2 MV(IV) solution in 4 M total sulfates with/without 0.05 M SPT and 2 MV(III) solution in 4 M total sulfates without SPT were used as positive and negative electrolytes, respectively. Fig. 8 shows the charge/discharge potential profiles at a current density of 40 mA cm^{-2} at 20°C. The potential cutoff was fixed at 1.6 V to avoid the evolution of H_2 and O_2. As can be seen in the profiles, the potential plateaus at ca. 1.5 V during charge and ca. 1.2 V during discharge represent the V^{4+}/V^{5+} vs. V^{2+}/V^{3+} redox reaction. It can be also seen that the charge/discharge time (i.e., capacity) of the cell without the additive remarkably decreases during cycling (Fig. 8(a)), while the charge/discharge time of the cell with the additive slightly decreases.

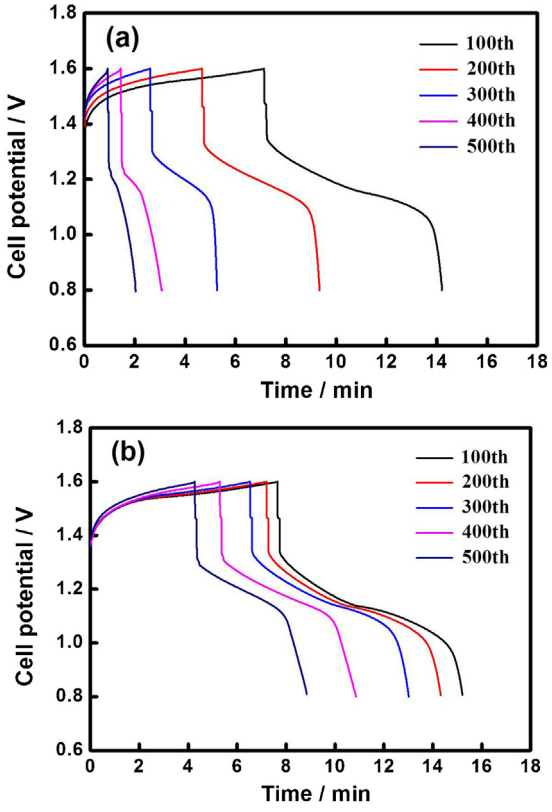

Fig. 8. Charge/discharge curves of VRFB non-flow cells without (a) and with (b) a SPT additive.

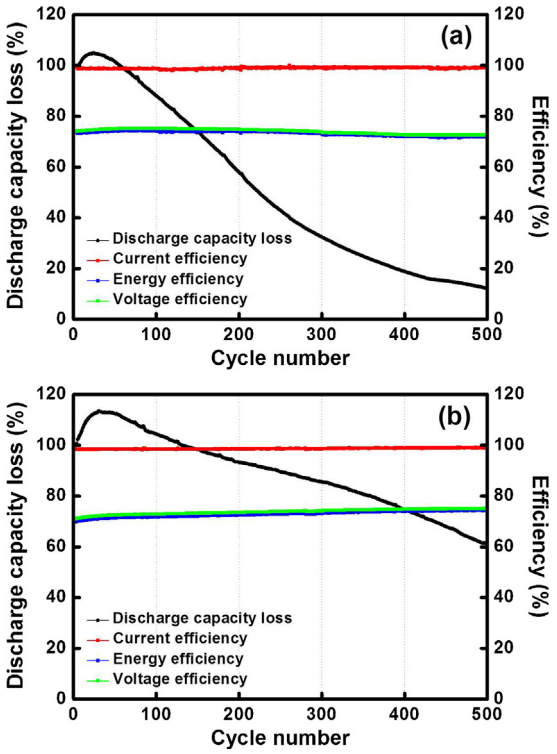

Fig. 9. Discharge capacity loss and efficiency of VRFB non-flow cells without (a) and with (b) a SPT additive as a function of cycle number at 20°C.

Fig. 9 shows the efficiencies and discharge capacity loss of VRFB single-unit cells. In general, CE, VE, EE, and discharge capacity are the most common categories used to evaluate the performance of VRFBs; these values can be derived from the charge/discharge curves [26]. The CE factor describes how well electrons are transferred into and out of the system; this factor can be used to track side reactions including self-discharge reactions resulting from diffusion of vanadium ions across the membrane, or other faradaic losses. Under fixed potential window and current density, CE values are determined by the ratio of the charge to the discharge time (or capacity). From the results shown in Fig. 9, it can be confirmed that CE values of both cells are as high as, or over, 98%. These high CE values may be attributed to the short charge/discharge time, which is the nature of non-flow cells with small volume (ca. 3 mL) of both electrolytes, as well as to an ion-exchange membrane with low vanadium permeability.

The VE factor describes losses through both overpotential and electrolyte imbalance caused by electrolyte crossover and is determined by the potential difference between the charge and discharge processes. The VE values of the cell without the additive decrease slightly during cycling, while those of the cell with the additive increase slightly, implying better cycling performance due to the addition of the SPT. It has been reported that cell resistance change between the charge and the discharge has an effect on the VE in the VRFB cell [27]. Therefore, the cell resistance was calculated from Eq. (4) in order to estimate its influence in the VE. As a result, it was observed that the resistance of the cell with an additive exhibits consistent values, while resistance of the cell without the additive increases slightly. This increase of cell resistance may be attributed to precipitates, which may block the pores of a membrane or reduce the surface area of the felt electrodes and cripple the pump circulation. In addition, the precipitates in

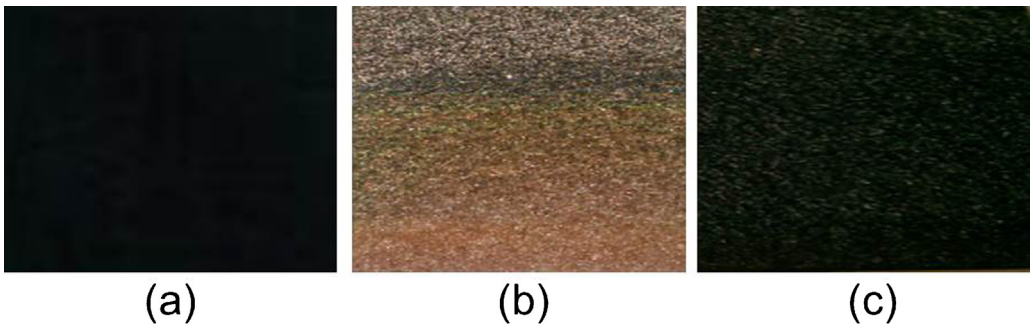

Fig. 10. The positive felt electrode of disassembled cells: pristine (a), without (b) and with (c) a SPT additive.

Table 1
Electrochemical performance of VRFB non-flow cells with and without a SPT additive.

Sample	Cycle (No.)	Discharge capacity loss (%)	CE (%)	VE (%)	EE (%)	Cell resistance (Ω)
No additive	100	88 ± 0.1	99 ± 0.1	75 ± 0.1	74 ± 0.2	0.25 ± 0.01
	200	58 ± 0.5	99 ± 0.2	75 ± 0.1	74 ± 0.3	0.27 ± 0.01
	300	32 ± 0.8	99 ± 0.3	74 ± 0.3	73 ± 0.5	0.29 ± 0.02
	400	19 ± 0.3	99 ± 0.2	73 ± 0.2	72 ± 0.3	0.31 ± 0.02
	500	12 ± 0.1	99 ± 0.3	73 ± 0.1	72 ± 0.3	0.32 ± 0.01
Additive (0.05 M SPT)	100	104 ± 2.8	99 ± 0.1	72.9	72 ± 0.4	0.25 ± 0.02
	200	93 ± 0.6	99 ± 0.1	73.2	72 ± 0.1	0.25 ± 0.02
	300	86 ± 1.1	99 ± 0.1	74.0	73 ± 0.3	0.26 ± 0.02
	400	75 ± 1.2	99 ± 0.1	75.0	74 ± 0.4	0.25 ± 0.01
	500	61 ± 2.0	99 ± 0.2	75.2	75 ± 0.3	0.26 ± 0.01

practical flow cells can block narrow manifolds, spoiling flow distribution. The EE factor reveals the overall efficiency of the VRFB as the product of CE and VE. The cell with an additive exhibited the highest EE value of 74.6% at the 500th cycle. For convenience of comparison, the main data are listed in Table 1.

The discharging capacity fading curves are also shown in Fig. 9. Though the cell (Fig. 9(b)) with an additive showed a gradual decrease in discharge capacity during cycling, its discharge capacity loss was remarkably lower than that of the cell (Fig. 9(a)) without the additive, suggesting good cycling stability. The key reason for the capacity fading over charge/discharge cycling includes not only the imbalanced vanadium active species caused by cross-contamination through the membrane, but also the loss of vanadium active species by precipitation [28].

In order to observe the precipitation features of the carbon felt electrode on the positive pole, the cell was disassembled after 500 charge/discharge cycles. As shown in Fig. 10(b), it is clear that there were a large number of V_2O_5 precipitation particles on the felt electrode from the cell without an additive. In addition, the felt electrode of the cell without an additive became more rigid because its pores were blocked by the precipitation particles. Meanwhile, the felt electrode of the cell with an additive had little precipitation (Fig. 10(c)). No precipitation was observed on the negative felt electrode from either the cells with and without an additive. This precipitation gives rise to an imbalance between the positive and negative half-cell electrolytes, which results in a significant capacity loss. From this result, it was concluded that primarily, it was V_2O_5 precipitation which directly affected capacity fading.

Overall, the cell using positive electrolytes containing the SPT additive exhibited better electrolyte stability and electrochemical performance compared with the blank one. However, the exact mechanism of stabilization by the SPT ($Na_4P_2O_7$) additive is not known yet. Skyllas-Kazocos and co-workers reported that sodium hexametaphosphate ($(NaPO_3)_6$) containing six phosphate groups in a ring was an effective precipitation inhibitor for supersaturated vanadyl sulfate solutions [16], reducing the precipitation rate of the vanadyl sulfate by adsorbing on the surface of the nuclei, thus reducing the rate of crystal growth. Extensive studies of precipitation inhibitors for V(V) solutions were also carried out by Skyllas-Kazacos and co-workers [14] who found a similar mechanism for V(V) precipitation inhibition. From these results, it is expected that the SPT additive will also reduce the precipitation rate of the vanadyl sulfate by adsorbing on the surface of the nuclei.

Further studies are needed to understand exactly the action of the SPT additive because this paper reports preliminary results only. In addition, a flow cell test is still needed to determine the effects of the additive on the stability of the other vanadium oxidation states, spoiling flow distribution, and over a wide operating temperature, even though the non-flow cell test showed a positive effect at room temperature. These results will be reported in the near future.

4. Conclusions

In this research, sodium pyrophosphate tetrabasic (SPT) was introduced as an inorganic additive to the positive electrolyte of VRFBs and its effects on long-term stability and electrochemical performance were investigated. It was found that the V(V) electrolytes with and without the additive started to precipitate after 24 and 6 days, respectively. The UV-vis and CV measurement also suggested that the addition of SPT could effectively delay the formation of precipitation in positive electrolytes, and no new substances were formed in V(V) electrolyte with a SPT additive. Therefore, long-term stability of the V(V) electrolyte was improved by SPT, as demonstrated by the stability test. More importantly, it was found that the VRFB non-flow cell employing a positive electrolyte with the SPT additive exhibited less discharge capacity fading during cycling in comparison to the pristine one. In addition, a relatively higher average energy efficiency value of 74.6% was obtained for the electrolyte with SPT, compared to 71.8% for the electrolyte without the additive, at the 500th cycle at 20°C. From disassembly of 500-cycled cells, it was confirmed that the cell with an additive showed

less V_2O_5 precipitation particles than the cell without an additive. Thus, the SPT behaved as a stabilizing agent and retarded the process of precipitation in V(V) electrolytes. Therefore, SPT could be an effective additive for the positive electrolyte of VRFBs under limited laboratory short-term and small-scale conditions. Further effort is needed to exactly understand the action of the SPT additive and to determine its effects on the performance of long-term charge-discharge for flow cells.

Acknowledgements

This work was supported by the National Research Foundation of Korea Grant funded by the Korean Government (MEST) (NRF-2011-C1AAA001-0030538).

References

[1] Z. Yang, J. Zhang, M.C.W. Kintner-Meyer, X. Lu, D. Choi, J.P. Lemmon, J. Liu, Electrochemical energy storage for green grid, Chemical Reviews 111 (2011) 3577–3613.
[2] B. Dunn, H. Kamath, J.-M. Tarascon, Electrical energy storage for the grid: A battery of choices, Science 334 (2011) 928–935.
[3] C. Koroneos, T. Spachos, N. Moussiopoulos, Exergy analysis of renewable energy sources, Renewable Energy 28 (2003) 295–310.
[4] J.E. Halls, A. Hawthornthwaite, R.J. Hepworth, N.A. Roberts, K.J. Wright, Y. Zhou, S.J. Haswell, S.K. Haywood, S.M. Kelly, N.S. Lawrence, J.D. Wadhawan, Empowering the smart grid: can redox batteries be matched to renewable energy systems for energy storage? Energy & Environmental Science 6 (2013) 1026–1041.
[5] P. Leung, X. Li, C. Ponce de León, L. Berlouis, C.T.J. Low, F.C. Walsh, Progress in redox flow batteries, remaining challenges and their applications in energy storage, RSC Advances 2 (2012) 10125–10156.
[6] C. Ding, H. Zhang, X. Li, T. Liu, F. Xing, Vanadium flow battery for energy storage: prospects and challenges, The Journal of Physical Chemistry Letters 4 (2013) 1281–1294.
[7] M. Skyllas-Kazacos, M., Rychick, R. Robins, All-vanadium redox flow battery, U.S. Patent 4786567 (1988).
[8] H. Kaneko, K. Nozaki, Y. Wada, T. Aoki, A. Negishi, M. Kamimoto, Vanadium redox reactions and carbon electrodes for vanadium redox flow battery, Electrochimica Acta 36 (1991) 1191–1196.
[9] M. Skyllas-Kazacos, C. Menictas, M. Kazacos, Thermal stability of concentrated V(V) electrolytes in the vanadium redox cell, Journal of The Electrochemical Society 143 (1996) L86–L88.
[10] B. Sun, M. Skyllas-Kazacos, Chemical modification of graphite electrode materials for vanadium redox flow battery application-part II. Acid treatments, Electrochimica Acta 37 (1992) 2459–2465.
[11] B. Sun, M. Skyllas-Kazacos, Chemical modification and electrochemical behavior of graphite fibre in acidic vanadium solution, Electrochimica Acta 36 (1991) 513–517.
[12] F. Rahman, M. Skyllas-Kazacos, Solubility of vanadyl sulfate in concentrated sulfuric acid solutions, Journal of Power Sources 72 (1998) 105–110.
[13] L.Y. Li, S. Kim, W. Wang, M. Vijayakumar, Z.M. Nie, B.W. Chen, J.L. Zhang, G.G. Xia, J.Z. Hu, G. Graff, J. Liu, Z.G. Yang, A stable vanadium redox flow battery with high energy density for large-scale energy storage, Advanced Energy Materials 1 (2011) 394–400.
[14] M. Skyllas-Kazacos, Secondary batteries: redox flow battery–vanadium redox, in: J. Garche, P. Moseley, Z. Ogumi, D. Rand, B. Scrosati (Eds.), Encyclopedia of Electrochemical Power Sources, Elsevier, 2009, pp. 444–453.
[15] M. Skyllas-Kazacos, M. Kazacos, Stabilized electrolyte solutions, methods of preparation thereof and redox cells and batteries containing stabilized electrolyte solutions, US Patent 6,143,443 (November 07, 2000).
[16] M. Skyllas-Kazacos, C. Peng, M. Cheng, Evaluation of precipitation inhibitors for supersaturated vanadyl electrolytes for the vanadium redox battery, Electrochemical and Solid-State Letters 2 (1999) 121–122.
[17] S. Li, K. Huang, S. Liu, D. Fang, X. Wu, D. Lu, T. Wu, Effect of organic additives on positive electrolyte for vanadium redox battery, Electrochimica Acta 56 (2011) 5483–5487.
[18] M. Kazacos, M. Skyllas-Kazacos, High energy density vanadium electrolyte solutions, methods of preparation thereof and all-vanadium redox cells and batteries containing high energy vanadium electrolyte solutions, U.S. Patent 7078123 (2006).
[19] S.-J. Seo, B.-C. Kim, K.-W. Sung, J. Shim, J.-D. Jeon, K.-H. Shin, S.-H. Shin, S.-H. Yun, J.-Y. Lee, S.-H. Moon, Electrochemical properties of pore-filled anion exchange membranes and their ionic transport phenomena for vanadium redox flow battery applications, Journal of Membrane Science 428 (2013) 17–23.
[20] J.-G. Kim, S.-H. Lee, S.-I. Choi, C.-S. Jin, J.-C. Kim, C-.H. Ryu, G.-J. Hwang, Application of Psf-PPSS-TPA composite membrane in the all-vanadium redox flow battery, Journal of Industrial and Engineering Chemistry 16 (2010) 756–762.
[21] M.J. Watt-Smith, P. Ridley, R.G.A. Wills, A.A. Shah, F.C. Walsh, The importance of key operational variables and electrolyte monitoring to the performance of an all vanadium redox flow battery, Journal of Chemical Technology and Biotechnology 88 (2013) 126–138.
[22] N.H. Choi, S.-K. Kwon, H. Kim, Analysis of the oxidation of the V(II) by dissolved oxygen using UV-visible spectrophotometry in a vanadium redox flow battery, Journal of The Electrochemical Society 160 (2013) A973–A979.
[23] M. Kazacos, M. Cheng, M. Skyllas-Kazacos, Vanadium redox cell electrolyte optimization studies, Journal of Applied Electrochemistry 20 (1990) 463–467.
[24] F. Rahman, M. Skyllas-Kazacos, Vanadium redox battery: positive half-cell electrolyte studies, Journal of Power Sources 189 (2009) 1212–1219.
[25] A. Pan, J.-G. Zhang, Z. Nie, G. Cao, B.W. Arey, G. Li, S.-Q. Liang, J. Liu, Facile synthesized nanorod structured vanadium pentoxide for high-rate lithium batteries, Journal of Materials Chemistry 20 (2010) 9193–9199.
[26] E. Agar, C.R. Dennison, K.W. Knehr, E.C. Kumbur, Open circuit voltage of vanadium redox flow batteries: discrepancy between models and experiments, Electrochemical Communications 13 (2011) 342–345.
[27] G.-J. Hwang, H. Ohya, Crosslinking of anion exchange membrane by accelerated electron radiation as a separator for the all-vanadium redox flow battery, Journal of Membrane Science 132 (1997) 55–61.
[28] S. Corcuera, M. Skyllas-Kazacos, State-of-charge monitoring and electrolyte rebalancing methods for the vanadium redox flow battery, European Chemical Bulletin 1 (2012) 511–519.